P. KOPAS, M. BLATNICKÝ, M. SÁGA, M. VAŠKO

ISSN 0543-5846
METABK 56(1-2) 99-102 (2017)
UDC – UDK 669.715:621.791.057:620.178.3:620.17=111

IDENTIFICATION OF MECHANICAL PROPERTIES OF WELD JOINTS OF AlMgSi07.F25 ALUMINIUM ALLOY

Received – Primljeno: 2016-08-08
Accepted – Prihvaćeno: 2016-11-25
Original Scientific Paper – Izvorni znanstveni rad

The aim of this paper is to present the analysis of selected mechanical properties of weld joints of AlMgSi07.F25 aluminium alloy. We will focus on the influence of the test bar neck shape on the tensile strength characteristics and the course of hardness in the weld joint cross-section. For the welding process using TIG (Tungsten Inert Gas) technology we considered AlSi5 as the additive material. This paper also includes a short study of numerical modelling of the test bar welding.

Key words: aluminium alloy, weld joints, fatigue life, mechanical properties, numerical modelling

INTRODUCTION

In technical practice we often encounter connecting machine components using various technologies into larger structural units. These joints are also subject to physical laws – they experience, for example, wear and fatigue, that is degradation or changes to their original properties. One of the technologies of creating firm permanent joints of materials is welding. Welding usually generates the same or even greater strength than that of the base material, which depends on the base material type.

The expansive development of materials is instrumental in the constantly increasing use of materials based on other chemical elements than iron. An example is the replacement of heavy structures by lighter ones that are made of materials with lower density. These include aluminium and its alloys that have a very favourable strength-to-density ratio. In terms of production volume, aluminium is number one in the world among non-iron metals [1].

MATERIAL OF THE TEST SPECIMENS

As an experimental material to perform multiaxial fatigue tests was chosen the EN AW 6063.T66 (AlMgSi07.F25) aluminium alloy with a normalised chemical composition. This material is used because of the increased use of aluminium alloys especially in the advanced automotive industry (Table 1).

The test material was supplied in the form of round bars that had a diameter of 10 mm and a length of 1 520 mm. The subsequent cutting using a BOMAR 1 300 band saw resulted in the blank dimensions suitable to produce a 150 mm long test specimen due to the geometry required for fixing the specimen to the test device.

Table 1 **Chemical composition of the test specimen / wt./%**

Si	0,2 – 0,6	Mg	0,45 – 0,9
Fe	0,35	Cr	0,10
Cu	0,10	Zn	0,10
Mn	0,10	Ti	0,10
other elements		max. 0,05 each max. 0,15 total	
Al		remaining	

Aluminium alloys are mostly low-alloyed. The solubility of alloying materials in aluminium is relatively low; therefore the number of technically usable alloys of one group is limited. Aluminium alloys contain also other alloying elements intentionally added to aluminium in order to improve its mechanical, physical, metallurgical and technological properties. The most frequently used alloying elements are Mn, Mg, Cu, Zn and Si.

Aluminium and aluminium alloys do not have recrystallisation transformation in the solid state. Therefore they cannot be normalised. Each heating of hardened aluminium alloys above 200 °C results in decreased strength and hardness. This decrease is more pronounced at higher temperatures of heating. At temperatures of heating above 400 °C the effect of hardening is completely lost, and the alloy hardness decreases to a value corresponding to its annealed state [2].

PRODUCTION TECHNOLOGY OF WELD JOINT

Welding is a metallurgical process in which permanent, un-dismountable connections are formed by the inter-atomic bonds between the welded parts directly or through an additive material during its heating, respectively plastic deformation. There is a large number of welding technologies to achieve high-quality weld joints. Therefore, the specimen production required a precise definition of the technology that would achieve optimal properties and characteristics affecting the fa-

P. Kopas, M. Blatnický, M. Sága, M. Vaško, University of Žilina, Faculty of Mechanical Engineering, Department of Applied Mechanics, Žilina, Slovak Republic

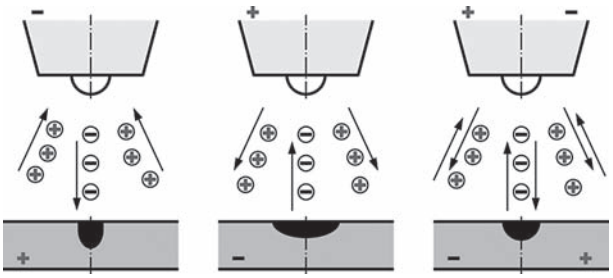

Figure 1 The principle of TIG welding at various connection polarities

tigue life. The authors chose the welding method using a non-melting tungsten electrode in an inert gas atmosphere – TIG.

In this welding technology an electric arc burns between the non-melting tungsten electrode and the base material in a protective argon atmosphere. This method is carried out at high temperatures, at which the joined materials are locally melted to the form a weld pool. TIG welding is most frequently used for welding Al, Mg and their alloys [3]. Aluminium and its alloys are welded only on alternating current with high-voltage or pulse ignition (Figure 1).

Weld ability of aluminium construction materials is evaluated according to selected indicators of weld joints, especially according to the indicator of integrity and the indicator of tensile strength of weld joints. After specification of the material to be welded we can propose an appropriate additive material and determine the optimal welding procedure. Table 2 shows the defined additive material.

To create a weld joint a Fronius Magic Wave 2 200 welding machine was used adhering to the following welding parameters: welding current I_z = 79 A, welding voltage U_z = 18,8 V, the tungsten electrode diameter d = 2,4 mm, the additive AlSi5 material diameter 2 mm, protective gas Ar 99.996% with the flow rate Q = 15 l·min^{-1}. This value of welding current was used because of stable burning of the electric arc during welding. A high value of current was not desirable, because the proportions of the weldment did not allow its heating to high temperatures due to the melting of the specimen entire metal volume.

Improving the properties of weld joints, i.e. especially their strength, was an important step in dealing with this issue. At the beginning of the fatigue test the residual strength value after welding is equal to the static strength of the test specimen. During the fatigue test there occurs degradation of residual strength [4]. At a certain time, the value of this parameter reaches the value of maximum possible load, and this causes the formation of a malfunction (fault). It is desirable to achieve a weld joint with a comparable strength of the base material, which is problematic in welding aluminium alloys.

The experiment consisted of performing the welding process with pre-heating and without pre-heating, slows cooling in the air, machining the specimens to the desired geometry for tensile tests, and comparing the results. The pre-heating temperature was 150 °C.

The first proposed alternative of the weld area – A-geometry is shown in Figure 2a. The disadvantage is in the frequent faults of weld joints – in particular root non-penetration. Also, there was no melting of the weld area. Only the additive material was melted, with minimum thickness after machining to the specimen geometry for fatigue assessment. This consisted of approximately 1 mm thick annular ring of additive material.

There was an attempt to change the weld area geometry. The first one was modified to a new B-geometry (Figure 2b). Since there was nore-boiling of the weld root and melting-down of the adjacent weld areas, the weldment was formed from one piece. Tensile strength after welding, with the above-mentioned weld area geometry, decreased significantly. The strength value was 129,1 MPa on average, which represents an average strength decrease by 12 % compared to the A-geometry. The weld joint started to feature other faults – inclusions resulting from the mixing of the weld metal with oxide films of Al_2O_3 when melting a small volume of metal that connected the two parts of the weldment. Inclusions caused the insufficient strength of the weld joint.

Another proposed specimen weld area (C-geometry) is based on the assumption that removing the base material situated at the point of the weld joint might lead to the elimination of occurrence of inclusions based on oxidic films; and complete removal of the height of blunting between the welded parts will ensure thorough penetration across the entire thickness of the weld (Figure 2c).

Tensile strength reached 166,4 MPa. The tabulated value of tensile strength for the base material AlMgSi07 is 247 MPa. This means that due to welding the strength decreased to 70 % of the original strength when welding with the C-geometry. After welding, this geometry showed the highest strength out of all the geometries used. Therefore, it was selected for weld testing using multiaxial fatigue tests [5].

The macrostructures of all three geometries fracture surfaces can be seen in Figure 3.

The specimens were machined to the desired geometry (Figure 4) in order to perform tensile testing. Tensile testing was extremely important for determining the weld joint strength, and also in subsequent investiga-

Table 2 **Applied additive material for welding**

Base material		Additive material	Joint tensile strength /MPa
Type	State		
AlMgSi	annealed	AlMg5, A1Si5	100 – 110
AlMgSi	hardened	AlMg5, A1Si5	110 – 120

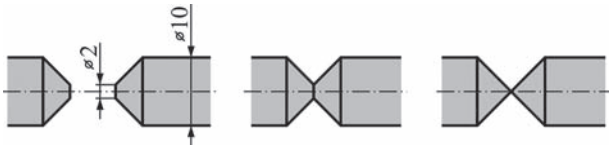

a) A-geometry b) B-geometry c) C-geometry

Figure 2 Geometry of the weld area

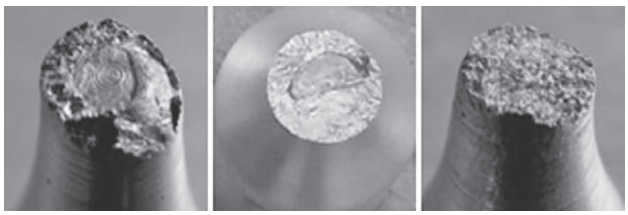

a) A-geometry b) B-geometry c) C-geometry
Figure 3 Macrostructure of fracture surfaces

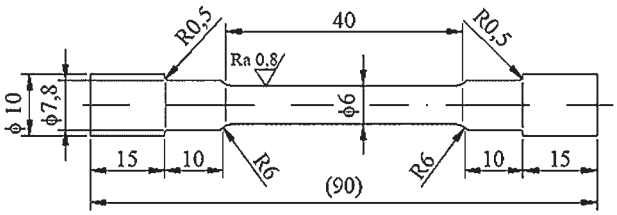

Figure 4 Specimen geometry for static tensile test

tions and calculations in the compilation of calibration curves for the test bench.

SPECIMEN MODELLING

The main objective of using numerical simulations of welding in industry is to determine the component deformations and the possibility of fault occurrence – based on the parameters such as material structure, hardness, residual stress and total plastic deformation. Furthermore, numerical simulations allow detailed understanding of the whole technological process, since they enable an insight into the results during the process (deformation, structure, stress, etc.), which is either not possible at all in the bulk of experimental measurements [6].

The first step was the creation of a Finite Element Method (FEM) model of the specimen welding process [7]. To address the above issue was used software called SysWeld that is one of the world's top software programs for complete solving of weld joint issues. After creating the FEM model of the weldment it was carried out a specimen welding simulation (Figure 5) [8].

The temperature at the point of contact of the electrode with the weldment at time t = 0,5 s reached the maximum value of 290 °C. At this time the so-far cold ends of the specimen had a temperature of 20 °C (i.e. the ambient temperature). In the course of another two seconds the maximum temperature at the welding reached

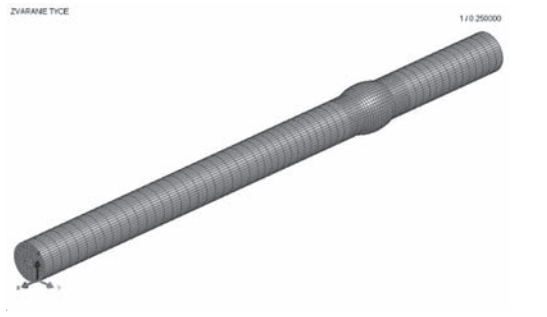

Figure 5 FEM model of the specimen weldment

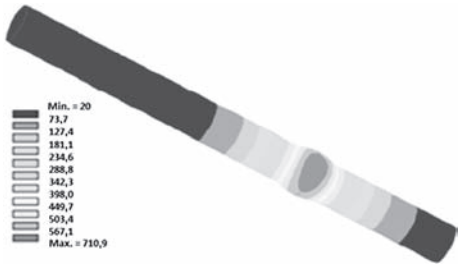

Figure 6 Heat propagation by conduction (t = 2,5 s)

711 °C. The temperature at the free ends was still relatively low. Heating of the free ends is indirect – generated by heat conduction in the material (Figure 6).

The specimen welding time as well as the specimen welding simulation time was 30 s. During this period, a weld joint was formed with strength of 166 MPa, which was proven by a tensile test. Immediately after welding, the maximum temperature was observed at the welding point, reaching 438,8 °C. The lowest temperature was observed at the longer side of the weldment from the weld, and it was 81 °C. The temperature courses were important data for assessing the size of the heat-affected area that played a role in measuring the hardness of individual areas of the weld joint.

The computational model was used to carry out analysis of displacements during the welding process, changes in different material phases due to the temperature, as well as detection of stress and deformations in real time. The largest displacement observed on the specimen during welding in the nodes is at time t = 30 s. The displacement value was 0,306 mm and the occurrence site was at the weld point.

During the welding process, material phases kept changing due to temperature and different chemical composition of the base and additive materials. The weld joint is formed by two semi-arched beads. Phase 1 represents the base material not affected by temperature during welding. Phase 2 is a representation of the welding metal and its affection by the temperature in weld bead 1. Simulation for phase 3 is similar, since we are dealing with a weld bead generated by the same welding technology. The last phase in the welding specimen is the heat-affected area (Figure 7). This is the area not melted by heat input from the welding process, but the temperature field achieved such robustness that the structure was modified [9]. This was proven by a change in hardness (Table 3), proving its decrease compared to the base material.

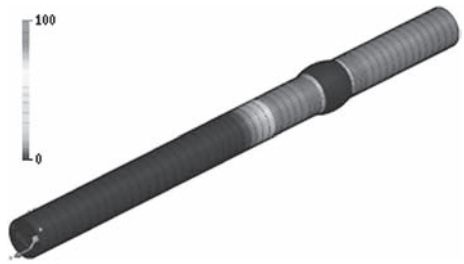

Figure 7 The percentage of the heat-affected area /%

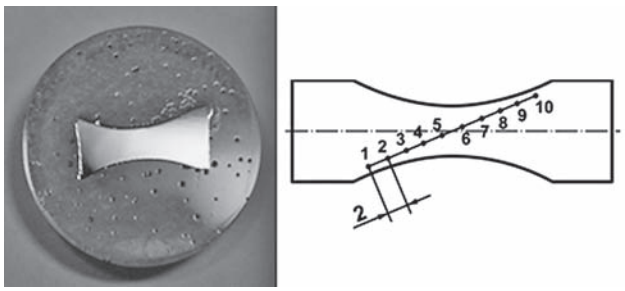

Figure 8 Specimen (left) and schematically plotted HV microhardness measurement position (right)

Table 3 **Specimen hardness measurement**

Hardness measurement point /HB			
No of measurement	Base material	Heat-affected area	Weld
1	61	52	46
2	69	46	48
3	65	50	48

The exact value of the AlMgSi07 hardness was determined by hardness measurement. It was employed Brinell measurement using a 5 mm diameter hard metal bead. Hardness measurements proved the material softening due to the input heat against the base material. Since the weld joint is not of the final specimen shape, this must be mechanically machined to a required geometry. Therefore, the specimen machining might have affected its hardness. The measured values have shown a moderate increase in microhardness close to the surface, compared to the specimen centre (Figure 8).

This may affect an increase in the specimen fatigue life, but not for comparison with a non-welded specimen because it was mechanically strengthened by machining [10]. For the comparison, the microhardness of pure iron is approximately 100 HV. The effect of machining can be captured at least partially in such a way that the surface may have been hardened by machining, which might increase the fatigue life [11]. It is therefore appropriate to measure microhardness near the surface and inside the weld joint (Table 4).

Table 4 **Hardness of the weld joint /HV**

No	1	2	3	4	5
HV	69	61	57	56	50
No	6	7	8	9	10
HV	56	54	59	60	63

CONCLUSIONS

The aim of this paper was to provide theoretical and practical preparation of specimen production for the multiaxial fatigue evaluation of weld joints. In order to evaluate multiaxial fatigue life, it was necessary to implement a weld joint with optimal mechanical properties into the specimen. That is why the initial selection of the material to be tested was followed by the selection of welding technology to be used to create the joint. The TIG method with alternating current was selected as the optimum technology. It has proven that the weld surface shape has the greatest impact on the strength.

A correct interpretation of the results of comparing the fatigue live of the base and welded materials requires a detailed explanation of all participating differences between specimen types. The differences that can be defined unambiguously include changes in the chemical composition due to the additive material, temperature and temperature field distribution due to welding, and the resulting change in the structure compared with the non-welded material. The welding process also causes residual stress that remains in the specimen and affects the fatigue life. Therefore, it will be appropriate to carry out numerical simulations to determine the residual stress values. The experiment unambiguously proved only a slight strengthening of the material just below the machined surface compared to the welded specimen cross-section centre.

Acknowledgements

This work was supported by the Slovak Research and Development Agency under the contract No. APVV-14-0096.

REFERENCES

[1] J. Belan, High frequency fatigue test of IN 718 alloy – microstructure and fractography evaluation. Metalurgija 54 (2015) 1, 59-62.
[2] G. Mathers, The welding of aluminium and its alloys. Woodhead Publishing, UK, 2002.
[3] M. Podrez-Radziszewska, Weldability problems of the technical AW7020 alloy. Manufacturing Technology 9 (2011) 11, 59-66.
[4] S. J. Maddox, Fatigue strength of welded structures. Woodhead Publishing, UK, 1991.
[5] D. Zhang, Y. Wang, Experimental investigation on fatigue damage rule of LY12CZ aluminum alloy under tension-torsion loading. Journal of Mechanical Strength 34 (2013) 5, 772-776.
[6] A. Sapietová, V. Dekýš, Dynamic analysis of rotating machines in MSC.ADAMS. Procedia Engineering 136 (2016), 143-149.
[7] K. J. Bathe, Finite Element Procedures. New Jersey, Prentice Hall, 1982.
[8] M. Žmindák, D. Riecky, Meshless Modelling of Laminate Mindlin Plates under Dynamic Loads. Communications 14 (2012) 3, 24-31.
[9] M. Vaško, M. Sága, Application of fuzzy structural analysis for damage prediction considering uncertain S/N curve. Applied Mechanics and Materials 420 (2013), 21-29.
[10] M. Sága, P. Kopas, M. Vaško, Some compu-tational aspects of vehicle shell frames optimization subjected to fatigue life. Communications 12 (2010) 4, 73-79.
[11] A. Vaško, L. Trško, R. Konečná, Fatigue behaviour of synthetic nodular cast irons. Metalurgija 54 (2015) 1, 19-22.

Note: The responsible translator for the English language is Mgr. J. Súkeníková, Žilina, Slovak Republic.